Anomalous in-plane magnetoresistance of electron-doped cuprate $La_{2-x}Ce_xCuO_{4\pm\delta}$

Yu Heshan, He Ge, Jia Yanli, Zhang Xu, Yuan Jie, Zhu Beiyi, Kusmartseva A., V. Kusmartsev F. and Jin Kui

Citation: SCIENCE CHINA Physics, Mechanics & Astronomy **60**, 097411 (2017); doi: 10.1007/s11433-017-9050-7

View online: http://engine.scichina.com/doi/10.1007/s11433-017-9050-7

View Table of Contents:http://engine.scichina.com/publisher/scp/journal/SCPMA/60/9

Published by the Science China Press

SCIENCE CHINA
Physics, Mechanics & Astronomy

SCIENCE CHINA
Physics, Mechanics & Astronomy

• Article •

September 2017 Vol. 60 No. 9: 097411
doi: 10.1007/s11433-017-9050-7

Anomalous in-plane magnetoresistance of electron-doped cuprate $La_{2-x}Ce_xCuO_{4\pm\delta}$

Heshan Yu[1,2], Ge He[1,2], Yanli Jia[1,2], Xu Zhang[1,2], Jie Yuan[1,3], Beiyi Zhu[1], A. Kusmartseva[4], F. V. Kusmartsev[4], and Kui Jin[1,2,3,5*]

[1] *Beijing National Laboratory for Condensed Matter Physics, Institute of Physics, Chinese Academy of Sciences, Beijing 100190, China;*
[2] *University of Chinese Academy of Sciences, Beijing 100049, China;*
[3] *CAS Key Laboratory of Vacuum Physics, University of Chinese Academy of Sciences, Beijing 100049, China;*
[4] *Department of Physics, Loughborough University, Loughborough LE11 3TU, UK;*
[5] *Collaborative Innovation Center of Quantum Matter, Beijing 100190, China*

Received May 1, 2017; accepted May 5, 2017; published online May 19, 2017

We report systematic in-plane magnetoresistance measurements on the electron-doped cuprate $La_{2-x}Ce_xCuO_{4\pm\delta}$ thin films as a function of Ce doping and oxygen content in the magnetic field up to 14 T. A crossover from negative to positive magnetoresistance occurs between the doping level $x = 0.07$ and 0.08. Above $x = 0.08$, the positive magnetoresistance effect appears, and is almost indiscernible at $x = 0.15$. By tuning the oxygen content, the as-grown samples show negative magnetoresistance effect, whereas the optimally annealed ones display positive magnetoresistance effect at the doping level $x = 0.15$. Intriguingly, a linear-field dependence of in-plane magnetoresistance is observed at the underdoping level $x = 0.06$, the optimal doping level $x = 0.1$ and slightly overdoping level $x = 0.11$. These anomalies of in-plane magnetoresistance may be related to the intrinsic inhomogeneity in the cuprates, which is discussed in the framework of network model.

electron-doped cuprates, negative magnetoresistance, linear magnetoresistance

PACS number(s): 73.50.-h, 74.78.-w, 74.25.Fy, 74.25.Dw, 74.72.-h

Citation: H. Yu, G. He, Y. Jia, X. Zhang, J. Yuan, B. Zhu, A. Kusmartseva, F. V. Kusmartsev, and K. Jin, Anomalous in-plane magnetoresistance of electron-doped cuprate $La_{2-x}Ce_xCuO_{4\pm\delta}$, Sci. China-Phys. Mech. Astron. **60**, 097411 (2017), doi: 10.1007/s11433-017-9050-7

1 Introduction

In order to understand the high-T_c superconductivity in the cuprates, it is necessary to study the unusual properties of the normal state by suppressing the superconductivity with magnetic field. Till now, many investigations of magnetoresistance (MR) are focused on the hole-doped cuprates to study properties of the normal state, i.e. the topology of Fermi surface [1,2], quantum criticality [3] etc. Compared with hole-doped cuprates, it is much easier to quench the superconductivity to study the normal state behaviors in the electron-doped counterpart [4,5]. Recently, low temperature negative MR (*n*-MR) effect was found in underdoped region of $Pr_{2-x}Ce_xCuO_{4\pm\delta}$ (PCCO), $Nd_{2-x}Ce_xCuO_{4\pm\delta}$ (NCCO) and $La_{2-x}Ce_xCuO_{4\pm\delta}$ (LCCO) in the case of B (magnetic field)$\perp ab$ plane (i.e. CuO_2 plane) [6-8]. Meanwhile, an upturn in temperature dependence of resistivity in the underdoped regime and metal-to-insulator transition near the optimal doping level were suggested to be related to the appearance of antiferromagnetic order with reducing temperature and doping, respectively [9-11]. When $B//ab$ plane, the in-plane MR showed two-fold symmetry in LCCO and coexistence of two- and four-fold symmetries in PCCO and NCCO, both

* Corresponding author (email: kuijin@iphy.ac.cn)

pointing to the antiferromagnetic order [12-14]. Neutron and transport studies on $Pr_{1.3-x}La_{0.7}Ce_xCuO_{4\pm\delta}$ (PLCCO) have revealed that the four-fold symmetric angular dependence is caused by a spin-flop transition, where the MR decreases as B//Cu-Cu direction, but increases as B//Cu-O-Cu direction [15]. Intriguingly, in both $B\perp ab$ plane and B//ab plane, a linear-field dependence of MR was observed at certain doping levels in PCCO, NCCO and LCCO systems [12,16,17], but the origin of the linearity is still under debate [18]. In addition to Ce doping, tuning oxygen by varying annealing procedures also has remarkable influence on the properties of normal state [4,19]. For instance, the crossover from n-MR to positive MR (p-MR) was found by reducing the oxygen concentration in NCCO [20,21]. Meanwhile the antiferromagnetic order fades away with increasing the annealing time [13,22]. Although fruitful MR anomalies in normal state of electron-doped cuprates have been unveiled, a systemic study on MR effects as a function of temperature, Ce, as well as oxygen in one system is still lacking.

In this paper, we present the in-plane MR of LCCO thin films in a wide range of Ce doping levels and oxygen content when B//ab plane. At x = 0.06 and 0.07, the optimally annealed samples (e.g. the samples which undergo the optimally annealing time) exhibit n-MR. The crossover from n-MR to p-MR occurs between x = 0.07 and 0.08. By varying the annealing processes, the in-plane MR of LCCO at x = 0.15 changes from n-MR (as-grown samples, which are not sufficiently annealed) to p-MR (the optimally annealed samples). Intriguingly, the linear MR is observed at the under-doping level x = 0.06, the optimal doping level x = 0.1 and slightly over-doping level x = 0.11.

2 Experimental methods

All the (00l) $La_{2-x}Ce_xCuO_{4\pm\delta}$ thin films were deposited directly on the (00l) $SrTiO_3$ substrates by the pulsed laser deposition technique at 700°C-750°C (ref. [12]). To achieve the highest T_{c0} (zero-resistance superconducting transition temperature) and sharpest transition width for different doping levels, we carefully adjusted the annealing process after the deposition. Then all the thin films (2000 Å) were patterned into a Hall-bar shape and measured in the Quantum Design PPMS 14T magnet at different angles between the magnetic field and the current (I). Measurements were taken with B//ab plane at 35 K to avoid influence from the superconducting fluctuations below 30 K [23,24]. By changing the annealing time, samples of different oxygen contents can thus be obtained.

3 Experimental results

Figure 1 displays the in-plane MR of LCCO thin films at 35 K with the Ce doping levels x = 0.06, 0.07, 0.08, 0.1, 0.11 and 0.15, respectively. In Figure 1(a) and (b), the optimally annealed samples show n-MR at x = 0.06 and 0.07. The crossover from n-MR to p-MR occurs between x = 0.07 and 0.08, in accordance with the boundary of static antiferromagnetic order achieved recently by the low energy μSR probe [25]. With further increasing Ce doping, the p-MR becomes indiscernible at x = 0.15 in Figure 1(c)-(f).

In Figure 2, the in-plane MR is plotted as a function of magnetic field at the doping level x = 0.15 subject to different annealing processes. In Figure 2(a), when the angles between the current and magnetic field are 0° (B//I) ,45° and 90° ($B\perp I$), the as-grown samples always show n-MR at 10 K. However, the short-annealed samples (e.g. the samples, of which annealing time is shorter than the optimally annealing time) exhibit n-MR in low magnetic field but p-MR above 13 T in Figure 2(b). For the optimally annealed samples, the in-plane MR shows p-MR in the case of B//I and $B\perp I$ (Figure 1(f)). The crossover from n-MR to p-MR is also observed by varying the annealing process.

Interestingly, negative linear MR is seen at the underdoping level x = 0.06 at 35 K in Figure 1(a). Similarly, positive linear in-plane MR occurs at the optimal doping level x = 0.1 and slightly overdoping level x = 0.11 in Figure 1(d) and (e). The linear in-plane MR of x = 0.1 is thoroughly investigated at θ = 30°, 45°, 60°, and 90°, as shown in Figure 3. Surprisingly, when the magnetic field was normalized by a sine function of the angle θ, the linear in-plane MR converged on a single straight line after subtracting the MR at B//I as shown in the inset of Figure 3. This means that only the perpendicular component of the field to the current direction contributes significantly to the linear MR. Similar linear MR is also observed in other electron-doped cuprates. For example, in PCCO and NCCO systems, the negative linear MR happens in the underdoped regime [16,17]. Meanwhile, near the optimal doping level, samples show positive linear MR in PCCO system [26].

Our findings can be summarized as follows: first, the crossover from n-MR to p-MR occurs between the doping level x = 0.07 and x = 0.08, in accordance with the boundary of static antiferromagnetic order achieved by the μSR (ref. [25]). Secondly, similar crossover from n-MR to p-MR occurs by varying the annealing process. Thirdly, the MR is linear and negative in field at the doping level x = 0.06, but positive at x = 0.1 and x = 0.11. Next, we will focus on the two fundamental phenomena: the n-MR and the linear MR.

4 Discussions

All the in-plane MR $\Delta\rho = \alpha B^{\gamma}$ in LCCO thin films are summarized in the Figure 4. In the extremely under-doped regime where the static antiferromagnetic order exists, the optimally annealed samples exhibit n-MR effect, as shown in the blue

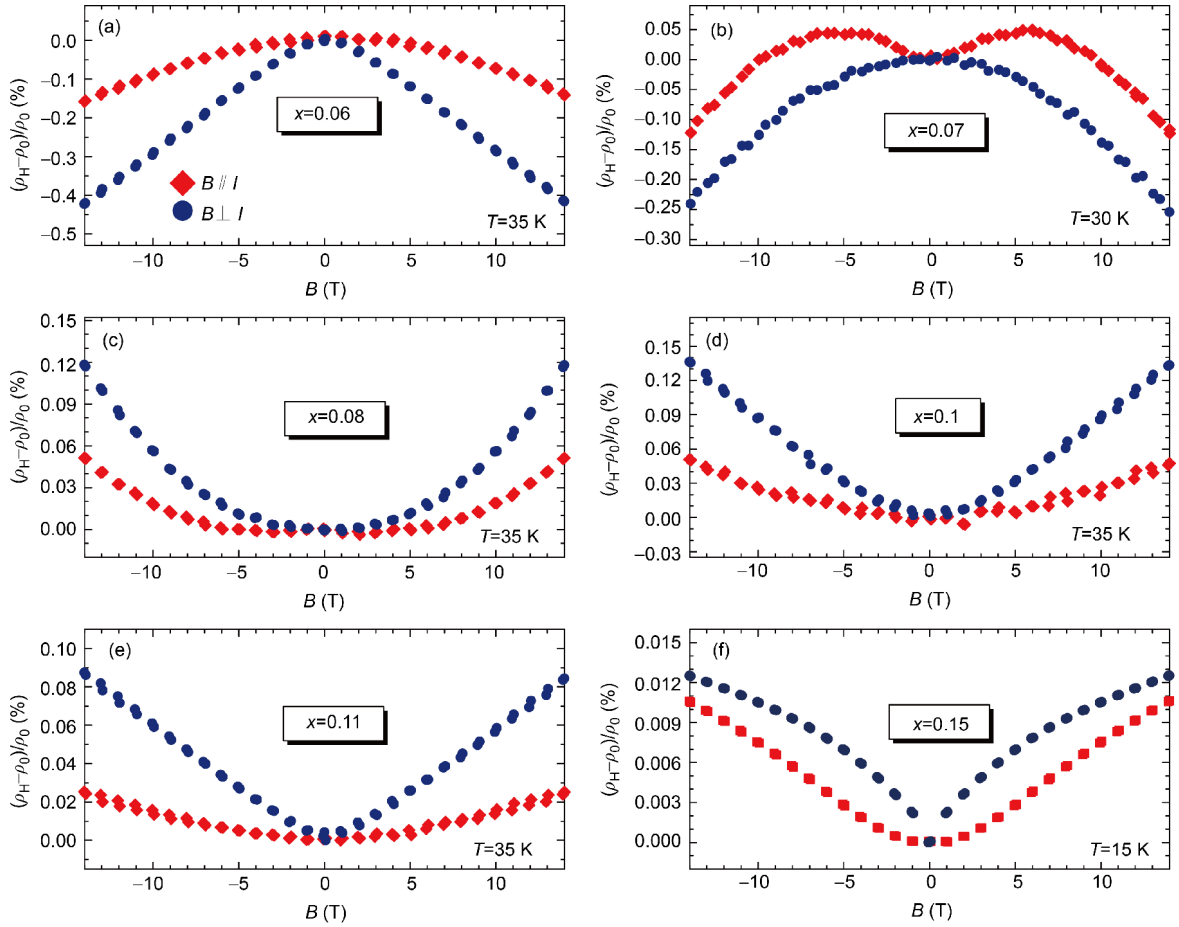

Figure 1 (Color online) The doping dependence of in-plane MR of optimally annealed LCCO in the normal state. In the doping level (a) $x = 0.06$, (b) $x = 0.07$, n-MR is observed with variation of magnetic field. At higher doping levels (c) $x = 0.08$, (d) $x = 0.1$, (e) $x = 0.11$ and (f) $x = 0.15$, p-MR is observed in the case of both $B//I$ and $B\perp I$.

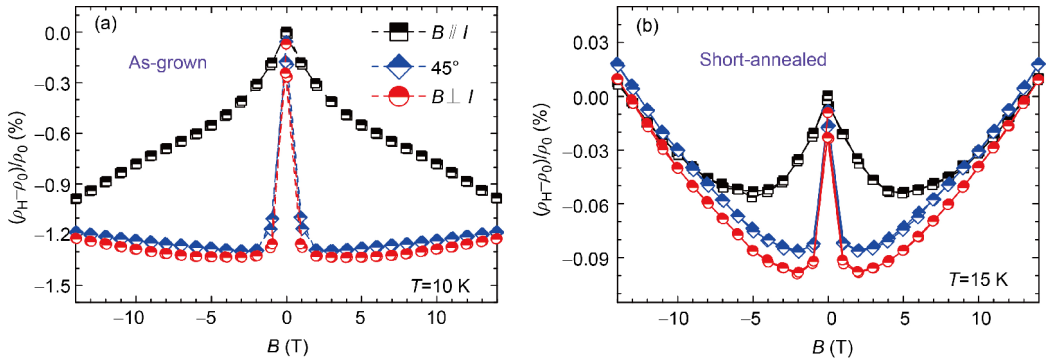

Figure 2 (Color online) The oxygen dependence of the in-plane MR at the doping level $x = 0.15$. When the angle θ between the magnetic field and the current is 0, 45° and 90°, (a) the as-grown films all show n-MR with the variation of magnetic field at $T = 10$ K; (b) the short-annealed films show n-MR behaviors in the low magnetic field but p-MR above 13 T.

area in Figure 4. Several studies propose that the origin of the n-MR may be related to the two-dimensional weak localization [7], Kondo scattering [6] or the conducting nano-filament (CNF) network model [27]. However, since there exists MR in the case of $B//ab$ plane, the two-dimensional weak localization seems not suitable here. Meanwhile, the existence of negative linear MR at $x = 0.06$ rules out the Kondo scattering, since the MR caused by the Kondo scattering usually has a logarithmic dependence on the magnetic field. By taking the simulations based on the CNF network, the n-MR is verified to exist with increasing magnetic field due to the spin polarizations (see the details in supplementary of ref. [24]). The framework of this CNF network as well as the n-MR caused by this network is discussed as follows. When an electron is doped on the Cu site, in order to decrease the on-site Hubbard repulsion, the charge density cloud of the doped electron will

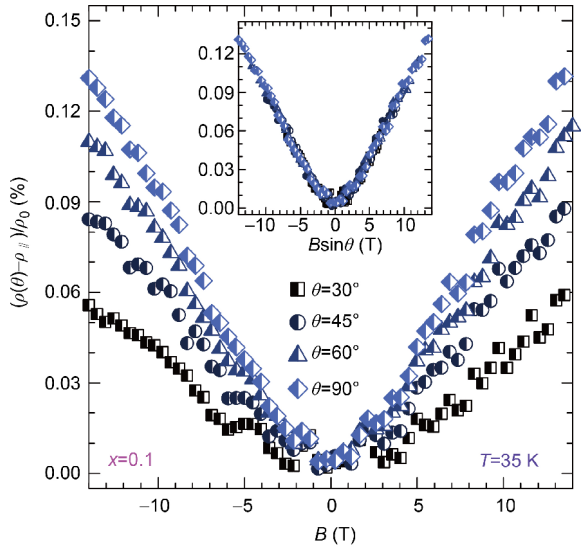

Figure 3 (Color online) The linear in-plane MR at the optimal doping level at $T = 35$ K. When $\theta = 30°$, 45°, 60°, and 90°, the in-plane MR is linear with the magnetic field. The illustration shows the normalization of MR: when the magnetic field was normalized by a sine function of the angle θ, the linear in-plane MR converges onto a single straight line.

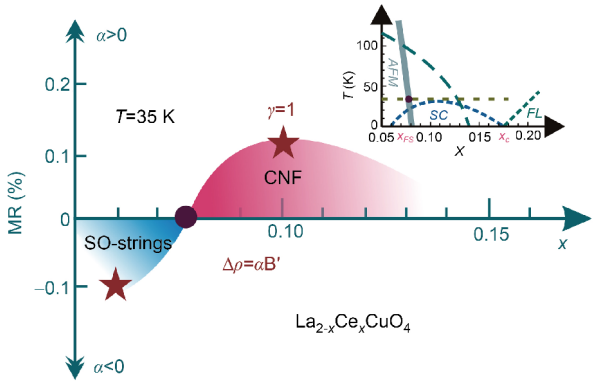

Figure 4 (Color online) The phase diagram of the electron-doped cuprate $La_{2-x}Ce_xCuO_4$ achieved by the in-plane MR at $T = 35$ K. At $x = 0.07$ and lower doping level, the n-MR is observed. The crossover from n-MR to p-MR occurs between $x = 0.07$ and 0.08 (marked by the purple dot in the illustration). Above $x = 0.08$, the p-MR occurs and almost vanishes at the doping level $x = 0.15$. At the doping levels $x = 0.06$, $x = 0.10$ and $x = 0.11$, the linear-field dependence of MR occurs. The illustration is the temperature-doping phase diagram of $La_{2-x}Ce_xCuO_4$. The boundary of static antiferromagnetic order (gray solid line) is achieved by the low energy μSR (ref. [25]). The green dash line is the boundary of dynamic antiferromagnetic order achieved by the AMR measurements. The light green dash line is the isotherm at 35 K in the phase diagram.

be shifted away from this copper site and even spreads around onto the neighbouring oxygen sites. That will be strongly polarizing the oxygen orbitals that are not taking part in the direct p-d electron bonding. This orbital polarisation may also involve the next-neighbouring oxygens and even further oxygens and result in the formation of polarization potential well for the considered doped electron. Then the doped electron may be self-trapped by this polarisation cloud (i.e. spin-orbital polaron) occupying several copper sites with same spin orientation. The spin-orbital (SO) polarons have a tendency to form clouds (or SO strings) inside of the antiferromagnetic background, which may have a quasi-one dimensional character to decrease the Coulomb repulsion between doped electrons in the cloud [28-30]. The doped electron could move along the one-dimensional channel inside these clouds of SO polarons. Owing to a small quantity of polarons, the static antiferromagnetic order could be stable up to the critical doping level $x = 0.08$. Antiferromagnetic order as well as the magnetic moment associated with the clouds is in the plane. The tunneling of the polarons between different planes is a rare event. Therefore, before the static antiferromagnetic order is destroyed, spins or magnetic moments inside these clouds of SO polarons are polarized due to the magnetic field. Such spin polarization decreases the spin scattering [31]. As a result, the n-MR effect occurs. It is similar to the n-MR behaviors in high magnetic field as $B \perp ab$ plane [32]. The n-MR signals are also very weak due to two reasons: a strong antiferromagnetic background where spins are located in the plane and a small number of SO polarons which form droplets decoupled from each other by the antiferromagnetic background.

With increasing the doping level, the SO polarons will also form a depletion that erases the interaction links in the antiferromagnetic lattice, and therefore weaken the antiferromagnetic interaction both between the planes and inside them. So there appear more and more erased moments. This frustration leads to the antiferromagnetic decoupling at some critical dopings. Then, due to these frustrations the static antiferromagnetic order vanishes at the critical doping level $x = 0.08$. It is detected by the μSR (ref. [25]) which is marked by the dot in the inset of Figure 4. The doping level $x = 0.08$ is a critical doping when the CNF is beginning to be formed. Effectively it is a percolation phase transition. When doping level is above 0.08, the percolation of SO polarons happens and each plane is conductive already. So the effect of spin polarization inside polarons is now very weak and become less important. As a result, the crossover from n-MR ($\alpha < 0$) to p-MR ($\alpha > 0$) occurs at this critical doping level. Consequently, the CNF network gives a plausible interpretation to the in-plane n-MR. Meanwhile, as shown in Figure 2(a) and (b), the as-grown and short-annealed samples show n-MR. This n-MR may be related to the existence of apical oxygen which could enhance the antiferromagnetic order inside samples [4]. On one hand, the suppressing of antiferromagnetic order by applied magnetic field could give rise to n-MR. On the other hand, according to the CNF network model, in the antiferromagnetic order regions, the CuO_2 plane becomes insulating. The doped electrons will move along the quasi-one dimensional channel inside the SO polarons. So the spins or magnetic moments inside SO polarons are polarized due to the magnetic field. Such polarization could give rise to n-MR,

similar to the *n*-MR behaviors at $x = 0.06$ and 0.07. As shown in Figure 1(b), there exits *p*-MR in low magnetic field in the case of $B//I$, but the origin needs further investigations.

Now we move to the second phenomenon: the linear MR, as shown in Figures 1(a), (d), (e) and 3. Till now, several models were proposed to explain the origin of linear MR, such as quantum MR [33], four-terminal resistor network [34], and density-wave transition [35], etc. Based on the assumption of a gapless spectrum with a linear momentum dependence, Abrikosov [33] proposed that linear quantum MR exists when system is in the limiting quantum case with electrons only occupying the lowest Landau level. But in PCCO, of which the properties are similar to LCCO, quantum oscillations only occur when the magnetic field is above 60 T [36]. That is, no Landau levels are formed in low magnetic field. Consequently, this model cannot explain the phenomenon of linear MR below 15 T in LCCO.

Parish and Littlewood [34] argue that if the sample is considered as a network consisting of four-terminal resistors, the linear MR could be from the Hall signal which is linear with magnetic field in an inhomogeneous system. In cuprates, both the rondom distribution of oxygen [37] and non-uniform magnetic response along the *c* axis [25] reveal the intrinsic inhomogeneity of the underdoped samples. So in LCCO, there may exist such four-terminal resistors between different CuO_2 planes. In this situation, there exists local current along the *c* axis, which could give rise to the Hall signals under in-plane magnetic field. These Hall signals are perpendicular to the magnetic field and in the *ab* plane. In extremely under-doped regime, both the Hall effects [38] and ARPES [39] show that there exists single electron band on the Fermi surface. These linear-field dependence of Hall signals contribute to linear in-plane MR. In the case of $B\perp I$, the linear-field dependence of Hall signal is along the current direction. Consequently, in this case the linear MR will be observed obviously, consistent with our observation that the linear MR is more dramatic in the case of $B\perp I$ at $x = 0.06$ as shown in the Figure 1(a), similar to the observation in non-magnetic silver chalcogenides [40]. That is, the negative linear MR may be dominated by the linear-field dependence of Hall signals. The four-terminal resistor network gives a plausible interpretation on negative linear MR at the doping level $x = 0.06$ in LCCO, as well as similar phenomena in the underdoped regime in other systems reported above [16,17]. However, it is still puzzling why the linear MR does not change sign as the direction of the magnetic field is reversed, which requests that the current along c axis should also change direction. Near the optimal doping level, the Hall signals are not linear with the magnetic field [27,38]. This means that only the four-terminal resistor network could not interpret the origin of this positive linear MR. Therefore, it needs further investigations to understand the origin of positive linear MR and why the linear MR is observed more dramatically in the case of $B\perp I$ as shown in the inset of Figure 3.

Otherwise, the linear MR is also verified to exist near the density wave (DW) transition where the Fermi surface is reconstructed and exhibits a local radius, i.e. cusp [35]. Here, the MR is dominated by a fraction of quasiparticle around the cusp, resulting in a nonanalytic response of linear MR. In LCCO, there exists spin density wave (SDW) transition near the optimal doping level (ref. [27]). However, such calculation near the DW transition is taken as $B\perp ab$ plane [35], it is unknown whether it works for the case of in-plane magnetic field or not.

5 Conclusions

In conclusion, we present a thorough study on the in-plane MR of LCCO thin films with the variation of Ce doping and oxygen content. By varying Ce doping, the crossover from *n*-MR to *p*-MR in the normal state occurs near the boundary of static antiferromagnetic order. The similar crossover is also observed by changing annealing process. In the extremely under-doped regime, optimally annealed samples exhibit *n*-MR, which may be interpreted by the CNF network model reasonably. Intriguingly, in the case of $B\perp I$, negative linear field-dependent MR is observed at $x = 0.06$, whereas positive linear field-dependent MR is investigated at $x = 0.1$ and $x = 0.11$. The four-terminal resistor network provides a plausible interpretation on the negative linear MR. Alternatively, the origin of positive linear MR near optimal doping level is unclear. These observations provide improved understanding and insights into the normal state properties in electron-doped cuprates.

The authors thank Prof. R. L. Greene for fruitful discussions. This work was supported by the National Key Basic Research Program of China (Grant Nos. 2015CB921000, and 2016YFA0300301), the National Natural Science Foundation of China (Grant Nos. 11674374, and 11474338), and the Key Research Program of Frontier Sciences, Chinese Academy of Sciences (Grant No. QYZDB-SSW-SLH008).

1 N. Doiron-Leyraud, C. Proust, D. Leboeuf, J. Levallois, J. B. Bonnemaison, R. Liang, D. A. Bonn, W. N. Hardy, and L. Taillefer, Nature **447**, 565 (2007), arXiv: 0801.1281.
2 B. Vignolle, A. Carrington, R. A. Cooper, M. M. J. French, A. P. MacKenzie, C. Jaudet, D. Vignolles, C. Proust, and N. E. Hussey, Nature **455**, 952 (2008).
3 R. A. Cooper, Y. Wang, B. Vignolle, O. J. Lipscombe, S. M. Hayden, Y. Tanabe, T. Adachi, Y. Koike, M. Nohara, H. Takagi, C. Proust, and N. E. Hussey, Science **323**, 603 (2009).
4 N. P. Armitage, P. Fournier, and R. L. Greene, Rev. Mod. Phys. **82**, 2421 (2010), arXiv: 0906.2931.
5 H. Yu, J. Yuan, B. Zhu, and K. Jin, Sci. China-Phys. Mech. Astron. **60**, 087421 (2017).
6 T. Sekitani, M. Naito, and N. Miura, Phys. Rev. B **67**, 174503 (2003).
7 P. Fournier, J. Higgins, H. Balci, E. Maiser, C. J. Lobb, and R. L. Greene, Phys. Rev. B **62**, R11993 (2000).
8 J. Yuan, G. He, H. Yang, Y. J. Shi, B. Y. Zhu, and K. Jin, Sci. China-

Phys. Mech. Astron. **58**, 107401 (2015).
9 P. Fournier, P. Mohanty, E. Maiser, S. Darzens, T. Venkatesan, C. J. Lobb, G. Czjzek, R. A. Webb, and R. L. Greene, Phys. Rev. Lett. **81**, 4720 (1998).
10 Y. Dagan, M. C. Barr, W. M. Fisher, R. Beck, T. Dhakal, A. Biswas, and R. L. Greene, Phys. Rev. Lett. **94**, 057005 (2005).
11 Y. Dagan, M. M. Qazilbash, C. P. Hill, V. N. Kulkarni, and R. L. Greene, Phys. Rev. Lett. **92**, 167001 (2004).
12 K. Jin, X. H. Zhang, P. Bach, and R. L. Greene, Phys. Rev. B **80**, 012501 (2009), arXiv: 0906.2974.
13 W. Yu, J. S. Higgins, P. Bach, and R. L. Greene, Phys. Rev. B **76**, 020503(R) (2007).
14 T. Wu, C. H. Wang, G. Wu, D. F. Fang, J. L. Luo, G. T. Liu, and X. H. Chen, J. Phys.-Condens. Matter **20**, 275226 (2008), arXiv: 0707.0104.
15 A. N. Lavrov, H. J. Kang, Y. Kurita, T. Suzuki, S. Komiya, J. W. Lynn, S. H. Lee, P. Dai, and Y. Ando, Phys. Rev. Lett. **92**, 227003 (2004).
16 T. Sekitani, H. Nakagawa, N. Miura, and M. Naito, Phys. B-Condens. Matter **294-295**, 358 (2001).
17 S. Finkelman, M. Sachs, G. Droulers, N. P. Butch, J. Paglione, P. Bach, R. L. Greene, and Y. Dagan, Phys. Rev. B **82**, 094508 (2010), arXiv: 1008.1682.
18 X. Zhang, H. Yu, G. He, W. Hu, J. Yuan, B. Zhu, and K. Jin, Phys. C-Supercond. Appl. **525-526**, 18 (2016), arXiv: 1602.08797.
19 J. S. Higgins, Y. Dagan, M. C. Barr, B. D. Weaver, and R. L. Greene, Phys. Rev. B **73**, 104510 (2006).
20 W. Jiang, S. N. Mao, X. X. Xi, X. Jiang, J. L. Peng, T. Venkatesan, C. J. Lobb, and R. L. Greene, Phys. Rev. Lett. **73**, 1291 (1994).
21 X. Q. Xu, S. N. Mao, W. Jiang, J. L. Peng, and R. L. Greene, Phys. Rev. B **53**, 871 (1996).
22 S. D. Wilson, S. Li, P. Dai, W. Bao, J. H. Chung, H. J. Kang, S. H. Lee, S. Komiya, Y. Ando, and Q. Si, Phys. Rev. B **74**, 144514 (2006).
23 P. Li, and R. L. Greene, Phys. Rev. B **76**, 174512 (2007), arXiv: 0708.1018.
24 Y. Dagan, M. M. Qazilbash, and R. L. Greene, Phys. Rev. Lett. **94**, 187003 (2005).
25 H. Saadaoui, Z. Salman, H. Luetkens, T. Prokscha, A. Suter, W. A. Macfarlane, Y. Jiang, K. Jin, R. L. Greene, E. Morenzoni, and R. F. Kiefl, Nat. Commun. **6**, 6041 (2015), arXiv: 1412.2775.
26 P. Li, F. F. Balakirev, and R. L. Greene, Phys. Rev. Lett. **99**, 047003 (2007).
27 H. Yu, G. He, Z. Lin, A. Kusmartseva, J. Yuan, B. Zhu, Y.-F. Yang, T. Xiang, L. Li, J. Wang, F. V. Kusmartsev, and K. Jin, arXiv: 1610.04788.
28 F. V. Kusmartsev, Phys. Rev. Lett. **84**, 530 (2000).
29 F. V. Kusmartsev, Phys. Rev. Lett. **84**, 5026 (2000).
30 F. V. Kusmartsev, J. Phys. **9**, 321 (1999).
31 M. Fath, Science **285**, 1540 (1999).
32 K. Jin, B. Y. Zhu, B. X. Wu, J. Vanacken, V. V. Moshchalkov, B. Xu, L. X. Cao, X. G. Qiu, and B. R. Zhao, Phys. Rev. B **77**, 172503 (2008).
33 A. A. Abrikosov, Phys. Rev. B **58**, 2788 (1998).
34 M. M. Parish, and P. B. Littlewood, Nature **426**, 162 (2003).
35 J. Fenton, and A. J. Schofield, Phys. Rev. Lett. **95**, 247201 (2005).
36 N. P. Breznay, I. M. Hayes, B. J. Ramshaw, R. D. McDonald, Y. Krockenberger, A. Ikeda, H. Irie, H. Yamamoto, and J. G. Analytis, Phys. Rev. B **94**, 104514 (2016), arXiv: 1609.00786.
37 M. Fratini, N. Poccia, A. Ricci, G. Campi, M. Burghammer, G. Aeppli, and A. Bianconi, Nature **466**, 841 (2010), arXiv: 1008.2015.
38 K. Jin, B. Y. Zhu, B. X. Wu, L. J. Gao, and B. R. Zhao, Phys. Rev. B **78**, 174521 (2008).
39 N. P. Armitage, F. Ronning, D. H. Lu, C. Kim, A. Damascelli, K. M. Shen, D. L. Feng, H. Eisaki, Z. X. Shen, P. K. Mang, N. Kaneko, M. Greven, Y. Onose, Y. Taguchi, and Y. Tokura, Phys. Rev. Lett. **88**, 257001 (2002).
40 R. Xu, A. Husmann, T. F. Rosenbaum, M. L. Saboungi, J. E. Enderby, and P. B. Littlewood, Nature **390**, 57 (1997).